

# The instability of a non-uniform vortex sheet

By L. M. HOCKING

University College London, Gower Street, W.C. 1

(Received 9 May 1963)

The classical Kelvin–Helmholtz problem of the instability of the vortex sheet between two uniform streams is extended to allow for non-uniformity in the streams. A small-wavelength approximation shows that the most unstable disturbances have a growth rate proportional to the greatest discontinuity of velocity at the vortex sheet. The solution for all wavelengths is found for two cases when the variation in the stream velocity is small compared with the stream velocity itself. One of these cases indicates that a transverse variation in the stream velocity can increase the instability for long wavelengths, but only to a small extent.

---

## 1. Introduction

Current interest in the behaviour of strong shear layers and vortex sheets has been stimulated by the leading edge vortex on a slender delta wing (Mangler & Smith 1959), and by the transition process in boundary-layer breakdown (Greenspan & Benney 1963). Flows of this kind are strictly three-dimensional, but a uni-directional and uniform velocity on either side of the layer or sheet is often used as a good local approximation. It is the purpose of this paper to discuss a slightly improved model, in which the flow is still uni-directional but non-uniform, and to find the effect of this non-uniformity on the instability of a vortex sheet.

Viscosity is neglected throughout this paper. The justification of this procedure is that what is under consideration is an extension of the classical, inviscid Kelvin–Helmholtz problem, to provide an initial study of a more general problem. The instability of a vortex sheet is an *inviscid* type of instability and a small viscosity in the fluid may be expected to make only a small change in its behaviour. There may be other, *viscous* modes of instability present and it is possible that these may be more unstable than the inviscid modes, as Brooke Benjamin (1963) has shown to be the case in another problem. On both sides of the vortex sheet, the fluid will be assumed to be moving in accordance with the Navier–Stokes equations to ensure that, when comparison is made with the behaviour of a real fluid, it is only at the vortex sheet itself that viscous forces will modify the undisturbed flow.

## 2. Analysis

The first step is to derive the inviscid Orr–Sommerfeld equation for a velocity  $W(x, y)$  in the  $z$ -direction, where  $(x, y, z)$  are Cartesian co-ordinates. In accordance with the standard procedure, the disturbance is supposed to have a real wave-

number  $\alpha$  in the  $z$ -direction and complex wave velocity  $c$  so that the velocity disturbance has the form  $(u, v, w) \exp\{i\alpha(z - ct)\}$ , where  $u, v, w$  are functions of  $x$  and  $y$  and are small compared with  $W$ . With a similar form for the pressure  $p$ , the linearized equations of motion and the continuity equation are

$$i\alpha(W - c)u = -p_x/\rho, \quad (1)$$

$$i\alpha(W - c)v = -p_y/\rho, \quad (2)$$

$$i\alpha(W - c)w + W_x u + W_y v = -i\alpha p/\rho, \quad (3)$$

$$u_x + v_y + i\alpha w = 0, \quad (4)$$

$\rho$  being the fluid density. Eliminating  $p$  and  $w$ , we obtain the two equations

$$(W - c)(u_{xx} - \alpha^2 u + v_{xy}) - W_{xx} u - W_{xy} v - W_y v_x + W_x v_y = 0, \quad (5)$$

$$(W - c)(v_{yy} - \alpha^2 v + u_{xy}) - W_{yy} v - W_{xy} u - W_x u_y + W_y u_x = 0. \quad (6)$$

If  $W$  is a function of  $x$  only and  $v = 0$ , these equations reduce to the well-known inviscid Orr–Sommerfeld equation.

For the particular problem of a vortex sheet, these equations must be solved on both sides of the sheet and the solutions matched by boundary conditions. To simplify the analysis, the value of the stream velocity on one side of the sheet will be assumed to be constant and, without further loss of generality, the fluid on this side can be taken to be at rest. The vortex sheet is in the plane  $x = 0$  and  $W(x, y)$  now refers to the velocity of the stream in the region  $x > 0$ ; for  $x < 0$ , equations (5) and (6) hold with  $W = 0$ .

The boundary conditions which must hold at the interface are continuity of normal velocity and pressure. If the displacement of the interface is

$$x = \xi(y) \exp\{i\alpha(z - ct)\},$$

the continuity of normal velocity requires that

$$u - i\alpha W \xi = -i\alpha c \xi$$

on both sides of the interface, or, in a form not involving  $\xi$ ,

$$\frac{u^{(1)}}{W - c} = \frac{u^{(2)}}{-c} \quad \text{at } x = 0. \quad (7)$$

The pressure can be found from (3) and the continuity of pressure condition is

$$(W - c)(u_x^{(1)} + v_y^{(1)}) - W_x u^{(1)} - W_y v^{(1)} = -c(u_x^{(2)} + v_y^{(2)}) \quad \text{at } x = 0. \quad (8)$$

Superscripts 1 and 2 refer to the regions  $x > 0$  and  $x < 0$ , respectively.

### 3. Small-wavelength approximation

When  $W$  is constant, the classical Kelvin–Helmholtz problem is obtained and the two possible values of  $c$  are

$$c = c_r + ic_i = \frac{1}{2}(1 \pm i)W, \quad (9)$$

and the growth-rate of the disturbance is  $\frac{1}{2}\alpha W$ . It is worth noting that this has the same value when the disturbance has a  $v$ -component, i.e. when the distur-

bance is moving at an angle to the main stream. For, if this angle is  $\beta$ , the velocity in this direction is  $W \cos \beta$  and the wave-number is  $\alpha \sec \beta$  so that  $\alpha c_i$  is unaltered. This is, of course, simply a special case of Squire's theorem on three-dimensional disturbances. The classical result shows that the most unstable disturbances are those with large  $\alpha$ , that is with small wavelength, and that the growth rate is proportional to the velocity discontinuity at the vortex sheet. This suggests that the solution in the more general case should be found for large  $\alpha$  if the most unstable disturbances are required.

With  $\alpha$  large, the terms of order  $\alpha^2$  in (5) and (6) are

$$u_{xx} - \alpha^2 u + v_{xy} = 0, \tag{10}$$

$$v_{yy} - \alpha^2 v + u_{xy} = 0, \tag{11}$$

and these equations have solutions, which satisfy the conditions of finiteness as  $x$  and  $y$  tend to infinity, of the forms

$$u^{(1)} = A^{(1)} \exp(-kx) \cos my, \quad v^{(1)} = A^{(1)}(m/k) \exp(-kx) \sin my, \tag{12}$$

$$u^{(2)} = A^{(2)} \exp(kx) \cos my, \quad v^{(2)} = A^{(2)}(-m/k) \exp(kx) \sin my, \tag{13}$$

where  $k^2 = m^2 + \alpha^2$ . Substituting these solutions in the conditions (7) and (8) gives

$$\{(W - c^2) + c^2\} u^{(1)}(0, y) = 0. \tag{14}$$

Since this equation is independent of  $k$ , it holds for any combination of the solutions (12), and so for any acceptable solution of (10) and (11). Remembering that the asymptotic solution for large  $\alpha$  is being sought, we see that (14) has the solution

$$u^{(1)}(0, y) = \delta(y - y_0), \tag{15}$$

where  $\delta$  is the Dirac  $\delta$ -function, provided

$$\{W(0, y_0) - c\}^2 + c^2 = 0.$$

The possible values of  $c$  are, therefore,

$$c = \frac{1}{2}(1 \pm i) W^i, \tag{16}$$

where  $W^i = W(0, y_0)$ , the value of  $W$  at the interface, and the greatest growth rate is

$$\frac{1}{2}\alpha \max(W^i). \tag{17}$$

The physical explanation of this result is clear. Consider a disturbance which is concentrated at a position  $y = y_0$ . Since the wavelength is very small any variation in the  $y$ -direction of the undisturbed flow will not be noticed and the disturbance will grow as if the whole stream were moving with the speed at the point  $(0, y_0)$ . Consequently, the largest growth rate will be the same as if the stream had a uniform velocity equal to its greatest speed at the interface.

Consider a fixed wave-number  $\alpha$  and suppose that at  $t = 0$ , the interface has a displacement  $\xi(y) \exp(i\alpha z)$ . Then at time  $t$  the displacement is

$$\begin{aligned} x &= \int_{-\infty}^{\infty} \xi(y_0) \delta(y - y_0) \exp\{i\alpha(z - ct)\} dy_0 \\ &= \xi(y) \exp\{i\alpha(z - \frac{1}{2}W^i t)\} \exp(\frac{1}{2}\alpha W^i t). \end{aligned} \tag{18}$$

This result shows how an initial disturbance changes its form and that non-linear effects will first become important at the points where  $W^i$  has its greatest value. It is at such points that turbulent spots may develop in the final stage of boundary-layer breakdown, when strong shear layers have been observed (see Greenspan & Benney 1963).

The reason why a continuous spectrum of values for  $c$  is obtained, instead of a single pair, is that the non-uniformity removes the degeneracy of the set of characteristic values of the uniform vortex sheet. In the classical problem, there is a continuous set of unstable characteristic solutions corresponding to plane disturbances propagating in different directions, which all have the same characteristic value. The effect of the non-uniformity is to destroy the two-dimensional nature of the solutions and to spread the degenerate set of characteristic values into a continuous spectrum.

#### 4. Nearly uniform stream

Although the greatest growth-rate of the disturbance is associated with large  $\alpha$ , it is of interest to find the effect of the non-uniformity of the stream for any  $\alpha$ , since in a viscous fluid the disturbances of very small wavelength are suppressed by viscous dissipation. The non-uniformity may be expected to have its greatest *relative* effect for small  $\alpha$ , or, more precisely, for disturbances whose wavelengths are greater than the length scale of variations in the main flow.

The mean value of the stream velocity may be taken as the unit of velocity, so that the stream velocity may be written  $W = W_0(1 + \tilde{W})$ , where the greatest value of  $\tilde{W}$  is small compared with 1.

To the first order in this small variation, the solution of (5) and (6) can be written

$$u^{(1)} = \phi_x^{(1)} + \tilde{W}_x \phi^{(1)} / (1 - c), \quad v^{(1)} = \phi_y^{(1)} + \tilde{W}_y \phi^{(1)} / (1 - c), \quad (19)$$

in the region  $x > 0$ , and

$$u^{(2)} = \phi_x^{(2)}, \quad v^{(2)} = \phi_y^{(2)}, \quad (20)$$

in the region  $x < 0$ , where  $\phi^{(1)}$  and  $\phi^{(2)}$  satisfy the equation

$$\phi_{xx} + \phi_{yy} - \alpha^2 \phi = 0. \quad (21)$$

This form of the solution is subject to the proviso that  $\tilde{W}$  satisfies the equation

$$\tilde{W}_{xx} + \tilde{W}_{yy} = 0.$$

This condition is that  $W$  must satisfy the Navier–Stokes equations in the region  $x > 0$  and is in agreement with the assumption stated in the introduction, designed to facilitate comparison with the behaviour of a viscous fluid.

The boundary conditions (7) and (8) to the first order become

$$\frac{(1 - c) \phi_x^{(1)} + \tilde{W}_x \phi^{(1)} - \tilde{W} \phi_x^{(1)}}{(1 - c)^2} = \frac{\phi_x^{(2)}}{-c} \quad \text{at } x = 0, \quad (22)$$

$$(1 - c) \phi^{(1)} + \tilde{W} \phi^{(1)} = -c \phi^{(2)} \quad \text{at } x = 0. \quad (23)$$

Since  $\phi^{(1)}$  must be bounded at  $y = \pm \infty$  and at  $x = +\infty$ , and  $\phi^{(2)}$  must be bounded at  $y = \pm \infty$  and at  $x = -\infty$ , the appropriate forms for these solutions of (21) are

$$\phi^{(1)} = \int_{-\infty}^{\infty} f^{(1)}(k) \exp \{iky - x(\alpha^2 + k^2)^{\frac{1}{2}}\} dk, \quad (24)$$

$$\phi^{(2)} = \int_{-\infty}^{\infty} f^{(2)}(k) \exp \{iky + x(\alpha^2 + k^2)^{\frac{1}{2}}\} dk. \quad (25)$$

Since  $\tilde{W}$  satisfies the equation  $\tilde{W}_{xx} + \tilde{W}_{yy} = 0$ , it can be written

$$\tilde{W} = \int_{-\infty}^{\infty} g(k) \exp (iky - kx) dk. \quad (26)$$

Substituting these values of  $\phi^{(1)}$ ,  $\phi^{(2)}$  and  $\tilde{W}$ , with  $x = 0$ , in (22) and (23) and using the convolution theorem we find that the equations satisfied by  $f^{(1)}$  and  $f^{(2)}$  are

$$\int_{-\infty}^{\infty} \exp (iky) \left[ -(\alpha^2 + k^2)^{\frac{1}{2}} (1-c) f^{(1)}(k) + \int_{-\infty}^{\infty} \{[\alpha^2 + (k-n)^2]^{\frac{1}{2}} - n\} g(n) f^{(1)}(k-n) dn + (\alpha^2 + k^2)^{\frac{1}{2}} [(1-c)^2/c] f^{(2)}(k) \right] dk = 0, \quad (27)$$

$$\int_{-\infty}^{\infty} \exp (iky) \left[ (1-c) f^{(1)}(k) + \int_{-\infty}^{\infty} g(n) f^{(1)}(k-n) dn + c f^{(2)}(k) \right] dk = 0. \quad (28)$$

These equations hold for all  $y$ , so the integrands must vanish. Also, the change in the behaviour of the unstable disturbance is required so that  $c$  can be written as  $\frac{1}{2}(1+i)(1+\tilde{c})$ , where  $\tilde{c}$  is small and  $\tilde{c}^2$  is neglected. Finally, eliminating  $f^{(2)}$  gives an integral equation for  $f^{(1)}$

$$2\tilde{c}f^{(1)}(k) = \int_{-\infty}^{\infty} \left[ 1 + \left( \frac{\alpha^2 + (k-n)^2}{\alpha^2 + k^2} \right)^{\frac{1}{2}} - \frac{n}{(\alpha^2 + k^2)^{\frac{1}{2}}} \right] g(n) f^{(1)}(k-n) dn. \quad (29)$$

The possible values of  $\tilde{c}$  are those for which this equation has solution  $f^{(1)}(k)$  corresponding to permissible values of  $\phi^{(1)}$ . If  $f^{(1)}$  is absolutely integrable in  $(-\infty, \infty)$ , the Riemann–Lebesgue theorem shows that  $\phi^{(1)}$  tends to zero as  $y$  tends to infinity. If  $f^{(1)}$  is unbounded at infinity, no acceptable values for  $\phi^{(1)}$  are possible.

To consider now a particular value for  $\tilde{W}$ , suppose that

$$\tilde{W}(x, y) = \lambda \cos my \exp (-mx),$$

which corresponds to a small periodic variation in the  $y$ -direction superimposed on the uniform stream in the region  $x > 0$ . By the use of the result

$$\exp (imy) = \int_{-\infty}^{\infty} \exp (iky) \delta(k-m) dk, \quad (30)$$

the value of  $g$  is

$$g(k) = \frac{1}{2}\lambda \{ \delta(k-m) + \delta(k+m) \}, \quad (31)$$

and the equation for  $\tilde{c}$  becomes the difference equation

$$2\tilde{c}f^{(1)}(k) = \frac{1}{2}\lambda \left[ 1 + \left( \frac{\alpha^2 + (k-m)^2}{\alpha^2 + k^2} \right)^{\frac{1}{2}} - \frac{m}{(\alpha^2 + k^2)^{\frac{1}{2}}} \right] f^{(1)}(k-m) + \frac{1}{2}\lambda \left[ 1 + \left( \frac{\alpha^2 + (k+m)^2}{\alpha^2 + k^2} \right)^{\frac{1}{2}} + \frac{m}{(\alpha^2 + k^2)^{\frac{1}{2}}} \right] f^{(1)}(k+m). \quad (32)$$

If we write  $\bar{c} = \lambda p$ ,  $k = mn$ ,  $\alpha = m\beta$  and  $f^{(1)}(k) = F(n)$  the equation has the simpler form

$$2pF(n) = \frac{1}{2} \left[ 1 + \left( \frac{\beta^2 + (n-1)^2}{\beta^2 + n^2} \right)^{\frac{1}{2}} - \frac{1}{(\beta^2 + n^2)^{\frac{1}{2}}} \right] F(n-1) \\ + \frac{1}{2} \left[ 1 + \left( \frac{\beta^2 + (n+1)^2}{\beta^2 + n^2} \right)^{\frac{1}{2}} + \frac{1}{(\beta^2 + n^2)^{\frac{1}{2}}} \right] F(n+1). \quad (33)$$

For large  $n$ , the solutions of this equation behave like the solutions of

$$2pF(n) = F(n-1) + F(n+1). \quad (34)$$

If  $p > 1$ , this equation has solutions of the form

$$F(n) = At_1^n + Bt_2^n, \quad (35)$$

where  $t_1$  and  $t_2$  are the roots of  $t^2 - 2pt + 1 = 0$  and  $A$  and  $B$  are arbitrary functions of period 1. Since one root is greater than 1 and one is less than 1, all solutions are unbounded as  $n$  tends to  $+\infty$  or to  $-\infty$ , and hence there are no acceptable values of  $\phi^{(1)}$ . If  $p < 1$ , the solution has the form

$$F(n) = A \cos n\alpha + B \sin n\alpha, \quad (36)$$

where  $p = \cos \alpha$ , and  $F$  is not absolutely integrable in  $(-\infty, +\infty)$ . It is clear from the value of  $g(k)$  for this example that the functions used must be interpreted as generalized functions, and in this context it is sufficient for  $F$  to be absolutely integrable in any finite interval and to have an asymptotic form  $\exp(i\gamma n)$  for some real  $\gamma$  to ensure that  $\phi^{(1)}$  tends to zero as  $y$  tends to  $\pm\infty$  (Lighthill 1958). The solution (36) has the correct asymptotic form, and the complete equation (33) has no singularities for finite  $n$ . Hence, any value of  $p < 1$  gives acceptable values of  $\phi^{(1)}$ . If  $p = 1$ , a solution of (33) is  $F(n) = 1$ , and this also gives an acceptable value for  $\phi^{(1)}$ . Thus the greatest possible value of  $p$  is 1, and the corresponding value of  $c$  is  $\frac{1}{2}(1+i)(1+\lambda)$ . The maximum growth-rate of a disturbance is  $\alpha \frac{1}{2} W_0(1+\lambda) = \frac{1}{2}\alpha \max(W^i)$ . This is the same result as that obtained for small wavelengths in the general case (equation (17)), so that for the particular value of  $W$  used in this section, the small-wavelength result holds for all wavelengths.

## 5. Uniform transverse shear

The expectation that the non-uniformity should have its greatest relative effect for large wavelengths was not realized for the particular velocity field examined above, as the relative effect was found to be independent of  $\alpha$ . An interesting example is provided by a linear transverse variation in the value of  $W$ , and this does demonstrate a dependence on the wavelength of the disturbance. It is necessary, however, to limit the flow in the  $y$ -direction, since otherwise the velocity difference at the vortex sheet will become indefinitely large as  $y$  tends to  $\pm\infty$ . If the flow is confined to the region between walls at  $y = 0$  and  $y = \pi$ , where the distance between the walls has been taken as  $\pi$  times the length scale and all lengths are now non-dimensional, the velocity distribution is

$$W(x, y) = W_0 \{ 1 + 2\lambda(y - \frac{1}{2}\pi) \}$$

with  $W_0$  the mean velocity as before, and  $\lambda$  is small compared with 1. The solution must now be expressed as a Fourier series instead of a Fourier integral because of the limited range of  $y$ , and the conditions of boundedness at  $y = \pm \infty$  are replaced by the conditions  $v = 0$  at  $y = 0$  and at  $y = \pi$ .

Slightly different forms of  $u$  and  $v$  are chosen for convenience, and the solutions of (5) and (6) are taken to be

$$u^{(1)} = \sum_{n=0}^{\infty} A_n \exp\{-(\alpha^2 + n^2)^{\frac{1}{2}} x\} \left[ \cos ny - \frac{2\lambda \sin ny}{n\pi(1-c+\bar{W})} \right], \quad (37)$$

$$v^{(1)} = \sum_{n=0}^{\infty} A_n n(\alpha^2 + n^2)^{-\frac{1}{2}} \exp\{-(\alpha^2 + n^2)^{\frac{1}{2}} x\} \sin ny, \quad (38)$$

$$u^{(2)} = \sum_{n=0}^{\infty} B_n \exp\{(\alpha^2 + n^2)^{\frac{1}{2}} x\} \cos ny, \quad (39)$$

$$v^{(2)} = \sum_{n=0}^{\infty} -B_n n(\alpha^2 + n^2)^{-\frac{1}{2}} \exp\{(\alpha^2 + n^2)^{\frac{1}{2}} x\} \sin ny. \quad (40)$$

These solutions satisfy the conditions at  $y = 0$  and  $y = \pi$  and at  $x = \pm \infty$ . It is worth noting that these are the *exact* solutions of (5) and (6), that is, they apply for any value of  $\lambda$ . The conditions (7) and (8) which hold at the interface  $x = 0$  give

$$\begin{aligned} \sum_{n=0}^{\infty} A_n (\alpha^2 + n^2)^{-\frac{1}{2}} \left[ \left\{ 1 - c + \frac{2\lambda}{\pi} (y - \frac{1}{2}\pi) \right\} \cos ny - \frac{2\lambda}{\pi n} \sin ny \right] \\ = \sum_{n=0}^{\infty} B_n c(\alpha^2 + n^2)^{-\frac{1}{2}} \cos ny, \end{aligned} \quad (41)$$

$$\begin{aligned} \sum_{n=0}^{\infty} A_n \left\{ 1 - c + \frac{2\lambda}{\pi} (y - \frac{1}{2}\pi) \right\}^{-2} \left[ \left\{ 1 - c + \frac{2\lambda}{\pi} (y - \frac{1}{2}\pi) \right\} \cos ny - \frac{2\lambda}{\pi n} \sin ny \right] \\ = \sum_{n=0}^{\infty} -B_n c^{-1} \cos ny. \end{aligned} \quad (42)$$

Expanding the second of these in powers of  $\lambda$  and retaining the terms of order  $\lambda$ , we get

$$\sum_{n=0}^{\infty} A_n (1-c)^{-2} \left[ \left\{ 1 - c - \frac{2\lambda}{\pi} (y - \frac{1}{2}\pi) \right\} \cos ny - \frac{2\lambda}{\pi n} \sin ny \right] = \sum_{n=0}^{\infty} -B_n c^{-1} \cos ny. \quad (43)$$

If  $(y - \frac{1}{2}\pi) \cos ny$  and  $\sin ny$  are expanded as half-range Fourier cosine series and the coefficients of  $\cos my$  in both sides of (41) and (43) are equated,  $B_m$  can be eliminated and an infinite set of equations for the  $A_n$  is obtained. With

$$(y - \frac{1}{2}\pi) \cos ny = -\frac{4}{\pi} \sum_{m=0}^{\infty} \beta_{mn} \cos my, \quad (44)$$

$$\frac{\sin ny}{n} = -\frac{4}{\pi} \sum_{m=0}^{\infty} \gamma_{mn} \cos my, \quad (45)$$

the equations are

$$\begin{aligned} \sum_{n=0}^{\infty} A_n \left[ (1-c) \left\{ (1-c)^2 + c^2 \right\} \delta_{mn} - \frac{8\lambda}{\pi^2} \beta_{mn} \left\{ (1-c)^2 \left( \frac{\alpha^2 + m^2}{\alpha^2 + n^2} \right)^{\frac{1}{2}} - c^2 \right\} \right. \\ \left. + \frac{8\lambda}{\pi^2} \gamma_{mn} \left\{ (1-c)^2 \left( \frac{\alpha^2 + m^2}{\alpha^2 + n^2} \right)^{\frac{1}{2}} + c^2 \right\} \right] = 0, \quad (m = 0, 1, 2, \dots), \end{aligned} \quad (46)$$

where  $\delta_{mn}$  is the Kronecker  $\delta$  and

$$\left. \begin{aligned} \beta_{mn} &= (m^2 + n^2)/(m^2 - n^2)^2, & \gamma_{mn} &= 1/(n^2 - m^2) & \text{if } n + m \text{ is odd, } m \neq 0, \\ &= 1/2n^2, & &= 1/2n^2 & \text{if } m = 0, n \text{ odd,} \\ &= 0, & &= 0 & \text{otherwise.} \end{aligned} \right\} \quad (47)$$

As before, to find the change in the behaviour of the unstable mode to order  $\lambda$ ,  $c$  can be replaced by  $\frac{1}{2}(1+i)(1+\lambda p)$  and  $\lambda^2$  neglected, and the equation for  $p$  is found by equating the infinite determinant of the coefficients in (46) to zero. To the order required,  $p$  only appears in the diagonal elements, so that the possible values of  $p$  are the latent roots of the matrix  $\mathbf{A}$ , whose elements are given by

$$A_{mn} = \frac{4}{\pi^2} \beta_{mn} \left\{ \left( \frac{\alpha^2 + m^2}{\alpha^2 + n^2} \right)^{\frac{1}{2}} + 1 \right\} - \frac{4}{\pi^2} \gamma_{mn} \left\{ \left( \frac{\alpha^2 + m^2}{\alpha^2 + n^2} \right)^{\frac{1}{2}} - 1 \right\}. \quad (48)$$

It should be noted that the first row and column of this matrix are given by  $m = 0$  and  $n = 0$ , respectively.

Alternate elements in each row and column of  $\mathbf{A}$  are zero, and it is easily proved that the latent roots form positive and negative pairs. The latent roots can therefore be found from the matrix  $\mathbf{A}^2$ , by taking both square roots of each of its latent roots. The standard procedure for finding the latent root of greatest modulus of a matrix is to multiply a column repeatedly by the matrix, the ratio of a particular element after  $n+1$  multiplications to its value after  $n$  multiplications tending to the required latent root as  $n$  tends to  $\infty$ . This procedure applied to  $\mathbf{A}$  gives elements which are alternately zero and the method fails, but it can be used for the matrix  $\mathbf{A}^2$ , so that the largest latent root of  $\mathbf{A}$  can be found. Since the matrix is infinite, the process must be carried out for successively larger finite matrices until a limiting value can be estimated, a rough justification of this process being that the matrix elements decrease quite rapidly away from the leading diagonal. The largest latent root of  $\mathbf{A}$  has been found by this procedure for a range of values of  $\alpha$  and the values obtained have been used in constructing figure 1. The two extreme cases of very large and very small  $\alpha$  can be dealt with separately. When  $\alpha$  is very large  $A_{mn} = 8\beta_{mn}/\pi^2$  and the above procedure produced the value 0.997 for the largest latent root. However, the root can be shown to be exactly 1, since the sum of the elements in each column is

$$\frac{8}{\pi^2} \sum_{m=0}^{\infty} \beta_{mn}$$

and by use of (44) with  $y = 0$ , this sum is 1 for all  $n$ , so that  $\pm 1$  is one pair of latent roots. The positive root makes the maximum growth rate  $\frac{1}{2}\alpha W_0(1+\lambda)$  and since the greatest value of  $W$  at the interface is  $W_0(1+\lambda)$ , it can be written  $\frac{1}{2}\alpha \max(W^i)$ , which again is the value for the greatest growth rate found by the small-wavelength approximation for any  $W$ . The accuracy of the value found by the numerical procedure indicates that sufficient accuracy has been used for values of  $\alpha$  which are not large.

The other extreme case is when  $\alpha$  is very small and (48) can no longer be used as some of the coefficients in (46) are  $O(1/\alpha)$ , so that it is not true that  $c$  is altered



by only a small amount even though  $\lambda$  is small. According to (46) the determinant of coefficients with the largest terms retained is

$$\begin{vmatrix} -2c^3 + O(c^2) & \frac{8\lambda c^2}{\pi^2} & 0 & \frac{8\lambda c^2}{3^2\pi^2} & \dots \\ -\frac{16\lambda c^2}{\pi^2\alpha} + O(c) & -2c^3 + O(c^2) & O(\lambda c^2) & 0 & \dots \\ 0 & O(\lambda c^2) & -2c^3 + O(c^2) & O(\lambda c^2) & \dots \\ -\frac{16\lambda c^2}{3\pi^2\alpha} + O(c) & 0 & O(\lambda c^2) & -2c^3 + O(c^2) & \dots \end{vmatrix} = 0. \quad (49)$$

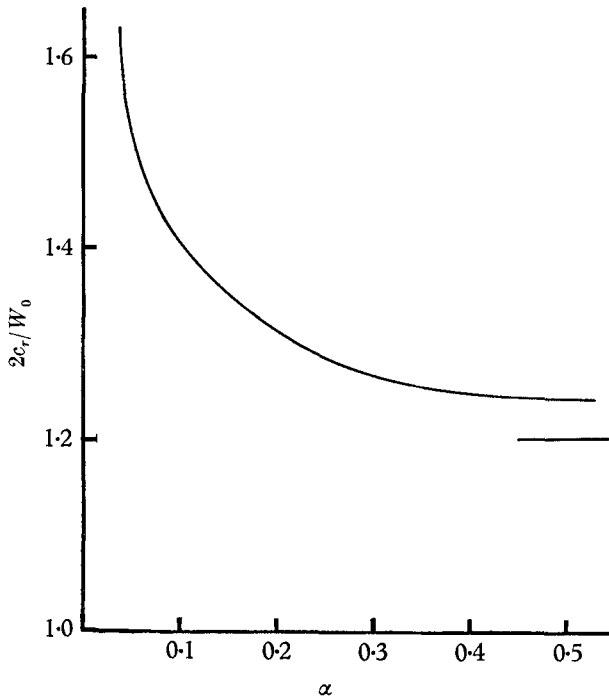


FIGURE 1. The phase velocity  $c_r$  ( $= c_i$ ) of disturbances to a vortex sheet with a transversely sheared stream on one side, with  $\lambda = 0.2$ .

The roots of this equation are  $O(1)$  except for one pair which are  $O(\lambda/\alpha^{1/2})$  and are given by

$$c^2 = -\frac{32\lambda^2}{\pi^4\alpha} \left( 1 + \frac{1}{3^3} + \frac{1}{5^3} \dots \right), \quad (50)$$

so that the maximum rate of growth when  $\alpha$  is small is  $0.578 \lambda \alpha^{1/2} W_0$ . These results for large and small  $\alpha$  are combined with the numerical results for intermediate values of  $\alpha$  to give figure 1, which illustrates the dependence of  $c_i$  (or  $c_r$ ) on  $\alpha$ , for the value  $\lambda = 0.2$ . The rate of growth for the most unstable disturbances is shown in figure 2, which also demonstrates how little it differs from the rate of growth for a uniform vortex sheet with a velocity discontinuity equal to the maximum velocity discontinuity of the non-uniform sheet. As was anticipated, the effect of the transverse variation is relatively largest for the longest waves and

it increases the instability of the flow, but the effect is very small and for most purposes it can be said that the maximum rate of growth is proportional to the wave-number and to the maximum velocity difference across the sheet, which was also found to be true for the periodic variation considered in the previous section.

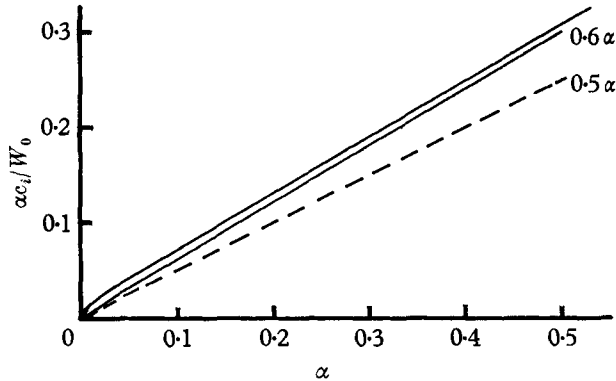


FIGURE 2. The maximum rate of growth of disturbances, for  $\lambda = 0.2$ . The full line gives the rate of growth for a uniform velocity  $W_0(1 + \lambda)$  and the broken line for  $\lambda = 0$ .

A less idealized approach to this problem would start with a shear layer instead of a vortex sheet and would include the effects of viscosity. The comparison between the uniform vortex sheet and the uniform shear layer with and without viscosity, given by Esch (1957), can be used to estimate the validity of the results obtained here. The shear layer differs from the vortex sheet in having a cut-off wave-number above which the motion is stable, and a maximum rate of growth at a finite wave-number. These wave-numbers decrease as the Reynolds number decreases and are based on the thickness of the shear layer as length scale. For shear layers whose thickness is much less than the distance between the walls, the left-hand portion of the curve in figure 2 will apply, but for large  $\alpha$  the curve will bend downwards and cut the axis, giving stability beyond that point. The effect of viscosity will be to give a similar curve with a lower rate of growth and wave-number, unless the interaction of viscosity and the non-uniformity introduces an unexpected effect.

This work was supported by a grant from the National Science Foundation to the Department of Engineering Mechanics, University of Michigan. The author wishes to express his gratitude to the Foundation and the Department, and, in particular, to Prof. C.-S. Yih for his encouragement and advice.

#### REFERENCES

- BENJAMIN, T. BROOKE 1963 *J. Fluid Mech.* **16**, 436.  
 ESCH, R. E. 1957 *J. Fluid Mech.* **3**, 289.  
 GREENSPAN, H. P. & BENNEY, D. J. 1963 *J. Fluid Mech.* **15**, 133.  
 LIGHTHILL, M. J. 1958 *Fourier Analysis and Generalized Functions*, p. 49. Cambridge University Press.  
 MANGLER, K. W. & SMITH, J. H. B. 1959 *Proc. Roy. Soc. A*, **251**, 200.